Forced underwater laminar flows with active magnetohydrodynamic metamaterials

Dean Culver and Yaroslav Urzhumov

Phys. Rev. E **96**, 063107 — Published 7 December 2017

DOI: 10.1103/PhysRevE.96.063107

Forced Underwater Laminar Flows with Active Magnetohydrodynamic Metamaterials

Dean Culver
Army Research Lab and Duke University Department of Mechanical Engineering and Materials Science

Yaroslav Urzhumov
Intellectual Ventures and Duke University Department of Electrical and Computer Engineering
(Dated: November 20, 2017)

Theory and practical implementations for wake-free propulsion systems are proposed and proven with CFD modeling. Introduced earlier, the concept of active hydrodynamic metamaterials is advanced by introducing magnetohydrodynamic (MHD) metamaterials, structures with custom-designed volumetric distribution of Lorentz forces acting upon a conducting fluid. Distributions of volume forces leading to wake-free, laminar flows are designed using multivariate optimization. Theoretical indications are presented that such flows can be sustained at arbitrarily high Reynolds numbers. Moreover, it is shown that in the limit $Re \gg 10^2$, a fixed volume force distribution may lead to a forced laminar flow across a wide range of Re numbers, without the need to reconfigure the force-generating metamaterial. Power requirements for such a device are studied as a function of the fluid conductivity. Implications to the design of distributed propulsion systems underwater and in space are discussed.

I. INTRODUCTION

Flow control is a subject of great interest in both aerospace and naval applications. Passive, or static, flow control measures date back to the work of Graham [1] (1952) and others, where wing geometry was optimized to maximize lift and minimize drag forces. Active methods, such as introduced flow [2] and sonic injection [3] were not far behind. The introduction of some flow potential in the boundary layer of an object in a fluid in particular became an area of great interest, such as in the work of Anderson [4], where the skin friction drag on long axisymmetric bodies is reduced through “laminarization” by manipulation of the boundary layer via area suction. Such studies (namely, those involving active control of a turbulent boundary layer for drag reduction) are prevalent in the literature even in recent years, such as in the work of Choi et al. [5] where a number of mechanical methods for controlling the boundary layer are studied via direct numerical simulation. Drag reduction is particularly important in hydrodynamics of underwater vessels, where energy efficiency of propulsion is directly linked to the effective drag coefficient of the vessel. In hydrodynamics, additional measures for reducing the skin drag are possible, such as supercavitation and polymer-injection techniques have been studied and, to some extent, reduced to practice.

However, until very recently, all aero- and hydrodynamic flow control measures have been limited to manipulating the boundary layer. With the advent of metamaterials [6, 7] and their ability to control various field distributions in all three dimensions, a question emerged whether controlling the flow volumetrically can lead to new modalities in flow control. A metamaterial is an artificially structured medium or structure that leverages field-matter interactions on a larger-than-molecular (such as mesoscopic or macroscopic) scale. A hydrodynamic metamaterial, in particular, leverages velocity and pressure fields by virtue of fluid-structure interactions. Unlike a porous medium, a hydrodynamic metamaterial has a precisely controlled (rather than stochastic or naturally emergent) structure of the solid and fluid particles. This question was answered positively in Refs. [8–10], where it was shown that fluid flows around obstacles can be “cloaked” (i.e. the wake behind the object is effectively eliminated) by an appropriate distribution of volumetric forces. Recent demonstrations of active metamaterials[11–17] stimulated the development of this concept for fluid dynamics, especially hydrodynamics.

Underwater vessels in particular are exposed to an interesting opportunity to produce volumetric force distributions, namely, the Lorentz force on charge carriers (ions) dissolved in naturally occuring water. Magnetohydrodynamic propulsion is being developed both for space vehicles as well as advanced surface or underwater vessels. On a smaller scale, it has been studied as a mechanism for flow control, for example, by Kim and Lee [18], who attempted to suppress the oscillatory force generated by vortex shedding using DC magnets and electrodes along a cylinder. In another work, Dennis et al. [19] show that MHD effects may be used to remove vortices from a diffuser.

In this work, we concentrate on the particular modality of flow control with active hydrodynamic metamaterials: wake elimination and suppression of turbulence by virtue of forcing a laminar flow pattern. The possibility of creating an unconditionally stable (i.e., laminar) flow around a cylinder at Reynolds numbers much greater than unity was hinted at in the work of Urzhumov and Smith[9]. Here, we present the theoretical basis for the existence of such flows at arbitrary Re, and prescriptions, including analytical formulas, for the requisite volume force distributions. Special attention is paid to the creation of forced Stokes flows, since the Stokes flow profile is the one that minimizes the total viscous dissipation in a stationary flow regime. Finally, we propose a materialization of the active metamaterial that would do this job — an MHD metamaterial that comprises interacting magnetic-field and electric-current generating elements. Furthermore, by virtue of optimization it is shown that the task of forcing a Stokes or another laminar flow pattern can be greatly simplified in comparison with the prescriptions given by the exact theory. A few-unit-cell active metamaterial is shown to reduce the wake by nearly an order of magnitude.

II. ZERO-WAKE AND FORCED STOKES FLOWS: THEORY AND DESIGN.

In general, when seeking solutions in terms of effective medium distributions, inverse problems are always nonlinear, even if the underlying equation is linear with respect to the field variables. However, when the volumetric source term itself is sought, the stationary solution is trivial, and is given by the stationary Navier Stokes equation

$$F = \rho\,(u \cdot \nabla)\,u - \mu\Delta u \tag{1}$$

where F is the volumetric force, ρ is the fluid density, u is the flow vector, and μ is the fluid viscosity. Here, the velocity distribution may be prescribed almost arbitrarily; it must only satisfy the continuity of velocity and stress. In this way, if we know the desired flow vector, we find an exact ”analytical” solution to the seemingly nonlinear problem.

We concentrate on the problem of stationary flow around a stationary-shape object, surrounded by a layer of a hydrodynamic metamaterial. The effect of the hydrodynamic metamaterial on the flow is modeled by the volumetric force term in the Navier-Stokes equation(s). This is similar to the Brinkman flow equation, as was done in [8, 9], albeit more direct and without introducing an intermediate quantity effective permeability tensor which links the body force and effective flow velocity. While generalizations can be easily made for fully three-dimensional objects (spherical or ellipsoidal), here we simplify the discussion by assuming that the object is an effectively infinite cylinder subject to a purely perpendicular flow. In applied hydrodynamics, conditions close to this simplified scenario can be found with long objects protruding down from a surface vessel, or in any direction from a submerged vessel. The radius of the cylinder is denoted r_c, and the outer radius of the active metamaterial layer is r_e.

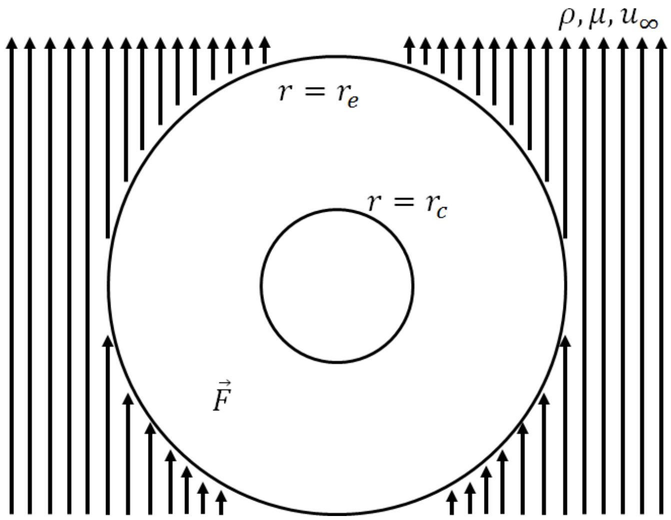

FIG. 1: Schematic of the annular cloak domain around a cylinder. The ideal cloak domain yields uniform flow for $r > r_e$.

We consider Reynolds numbers of the form $Re = \frac{\rho u_\infty d}{\mu}$ where ρ is the fluid density, u_∞ is the free-stream velocity, d is twice the core radius, and μ is the fluid viscosity. We seek configurations of this system that yield no wake, or flow perturbations due to the core geometry. Wake, defined point-wise as the Local Wake (LW) is defined as

$$LW \equiv \frac{|\vec{u} - u_\infty \hat{e}_f|}{u_\infty} \tag{2}$$

where $\hat{e}_f$ is the unit vector in the direction of the flow. The bulk disturbance in the flow is the Near-Field Wake (NFW) which is defined as

$$NFW = \frac{1}{2\pi r_e u_\infty} \oint_{s_{NF}} |\vec{u} - u_\infty \hat{e}_f| \, ds_{NF} \tag{3}$$

Where s_{NF} is along a circle of radius $r_{NF} = 1.1 r_e$ encompassing the cloak envelope.

We will approach this cloaking problem from several angles. First, we report a novel technique for identifying the force distribution necessary to achieve what we call a "forced Stokes flow". Secondly, we use optimization of a general volumetric force in the cloak envelope to achieve no wake. To best understand the values for the volumetric forcing necessary for cloaking, volumetric force values will be normalized against the drag force if it was distributed in the cloaking envelope. Namely, if the area of the envelope A_e is $A_e = \pi \left(r_e^2 - r_c^2\right)$, then we define a reference volumetric force value as

$$F_{V,0} \equiv \frac{\rho u_\infty^2 r_c}{\pi \left(r_e^2 - r_c^2\right)} \tag{4}$$

Knowing that the drag per unit depth for such a cylinder in high Reynolds number flow is

$$F_d = \frac{1}{2} \rho u_\infty^2 d C_d \tag{5}$$

where $C_d = 1$. Finally, we will explore design options leveraging magnetohydrodynamics to reduce the wake.

A. Zero-Wake Ansatz: Polynomials

Consider incompressible Stokes-Oseen flow in two dimensions, where a scalar stream function ψ can be used.

$$\psi = \hat{e}_z \cdot \nabla \times u \tag{6}$$

Require that the force field has a finite support domain. We choose an annulus for simplicity where F is nonzero on $\{r : r_c \leq r \leq r_e\}$. In order for an object to be "hydrodynamically cloaked", several criteria must be met. First of all, the flow field outside of the cloak domain must adhere to plug flow. Namely,

$$u = u_0 \hat{e}_y \rightarrow \psi = -u_0 r_e f\left(r\right) \sin\theta \tag{7}$$

where θ is measured from the positive y direction. Furthermore, we require no-slip at the inner boundary $r = r_c$ and velocity continuity at $r = r_e$. As long as these boundary conditions are satisfied, any velocity distribution may be prescribed in the annulus. Consider a polynomial ansatz solution

$$f_p\left(r\right) = \sum_{n=1}^{N} a_n \left(\frac{r - r_c}{r_e - r_c}\right)^n \tag{8}$$

If $N = 3$, we may satisfy all of the boundary conditions, where

$$a_1 = 0 \quad a_2 = 2 + \tfrac{r_c}{r_e} \quad a_3 = -1 - \tfrac{r_c}{r_e} \tag{9}$$

We substituted the resulting force distributions and solved the nonlinear Navier-Stokes system numerically. This three-term polynomial generates the flow field pictured in figure 2 in an annulus with an aspect ratio of $\gamma = \frac{r_c}{r_e} = 2$.

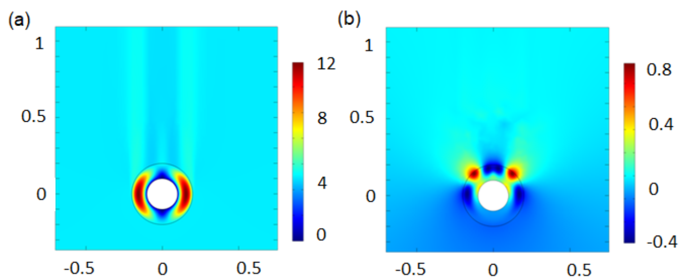

FIG. 2: Flow velocity (a) and pressure (b) as prescribed by a three-term polynomial ansatz for Re=10^3.

However, this solution yields a viscous stress discontinuity at the outer limit of the annulus, creating pressure discontinuities. In order to eliminate this, a four-term polynomial is used, where

$$a_1 = 0 \quad a_2 = 3\left(\gamma + 1\right) \quad a_3 = -3 - 5\gamma \quad a_4 = 2\gamma + 1 \tag{10}$$

This four-term polynomial generates the flow field pictured in figure 3 in an annulus with an aspect ratio of $\gamma = \frac{r_c}{r_e} = 2$.

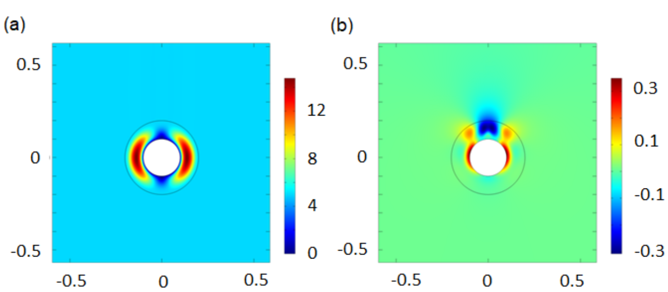

FIG. 3: Flow velocity (a) and pressure (b) as prescribed by a four-term polynomial ansatz for Re=10^3.

The results reported in figures 2 and 3 are computed using COMSOL multiphysics, computing the flow fields from the ansaetze prescribed by equations 9 and 10, respectively.

As there are an infinite number of solutions, we may choose another criterion to optimize the flow further. Consider the total work done by the volumetric force per unit time (i.e. mechanical power consumption).

$$W = \int (F \cdot u)\, dV = F_D u_\infty \tag{11}$$

where W is the mechanical work done, V is the volume of the cloak domain, F_D is the drag force, and u_∞ is, once again, the free stream velocity. For stationary incompressible flow, this is precisely the total energy dissipation rate through viscous loss.

$$W = \int (F \cdot u)\, dV = \int \mu\omega^2 dV \tag{12}$$

where ω is the vorticity. By energy minimization, this functional is minimized by the free Stokes flow satisfying the required boundary conditions. Thus the optimum prescribed velocity distribution is the one of Stokes flow, constrained by two interior and exterior boundary conditions on the domain of the volumetric force F. For the circular annulus, the (unique) solution is given by

$$f(r) = c_1 \frac{r_c}{r} + c_2 \frac{r}{r_c} + c_4 \left(\frac{r}{r_c}\right)^3 + c_3 \frac{r}{r_c} \ln \frac{r}{r_c} \tag{13}$$

where c_1 through c_4 may be determined from the four boundary conditions on u. Total dissipated power (and thus effective drag) was computed analytically for these forced Stokes flows

$$F_D \equiv \frac{W}{u_\infty} = 4\pi\mu u_\infty \Phi(\gamma) \tag{14}$$

where

$$\Phi = \frac{1+\gamma^2}{1-\gamma^2+(1+\gamma^2)\ln\gamma} \tag{15}$$

The function Φ is illustrated in figure 4 for a range of cloak aspect ratios.

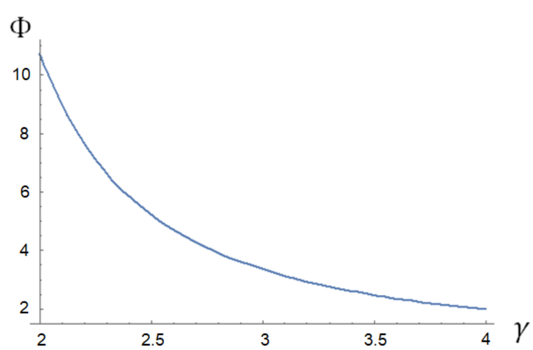

FIG. 4: Function Φ for a range of aspect ratios γ.

In the forced stokes flow, the system experiences effective drag with a linear dependence on velocity, but the uncloaked cylinder drag scales quadratically with velocity! This tells us that for any Re, there is a break-even aspect ratio γ_b such that for $\gamma > \gamma_b$ effective drag is less than the uncloaked cylinder drag. Our main conclusion, therefore, is that volumetric (3D distributed) propulsion systems may be able to achieve higher energy efficiency than a single-thruster or a boundary-distributed system provided that the thrust elements have (1) sufficiently small self-drag and (2) thrust generation efficiency is at least as good as conventional propellers with motors.

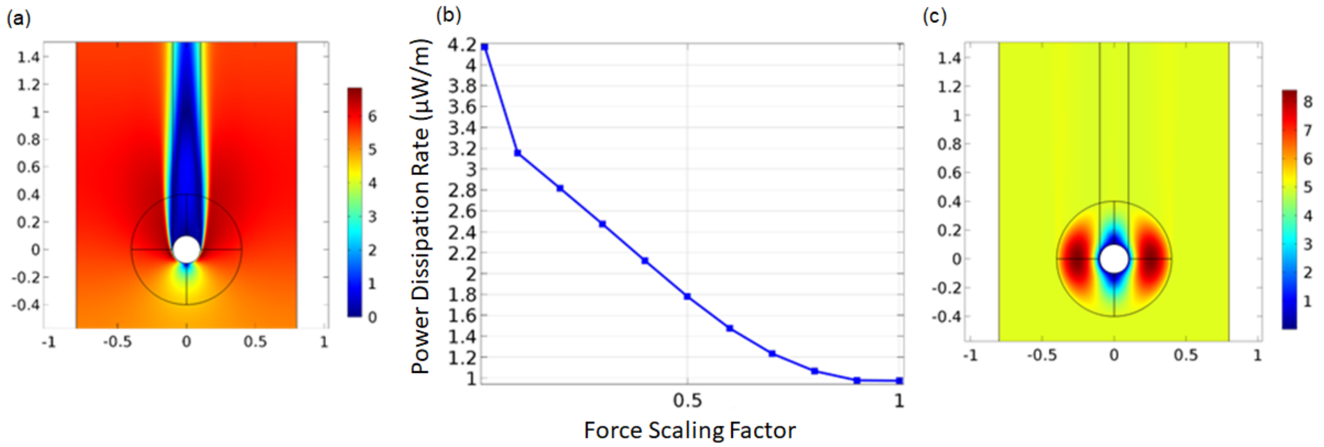

FIG. 5: (a - left) Flow field around an uncloaked cylinder. (b - center) Power dissipation for different volumetric force scaling factors, i.e. how "turned on" is the volumetric force. (c - right) Flow field around a cloaked cylinder using forced Stokes flow.

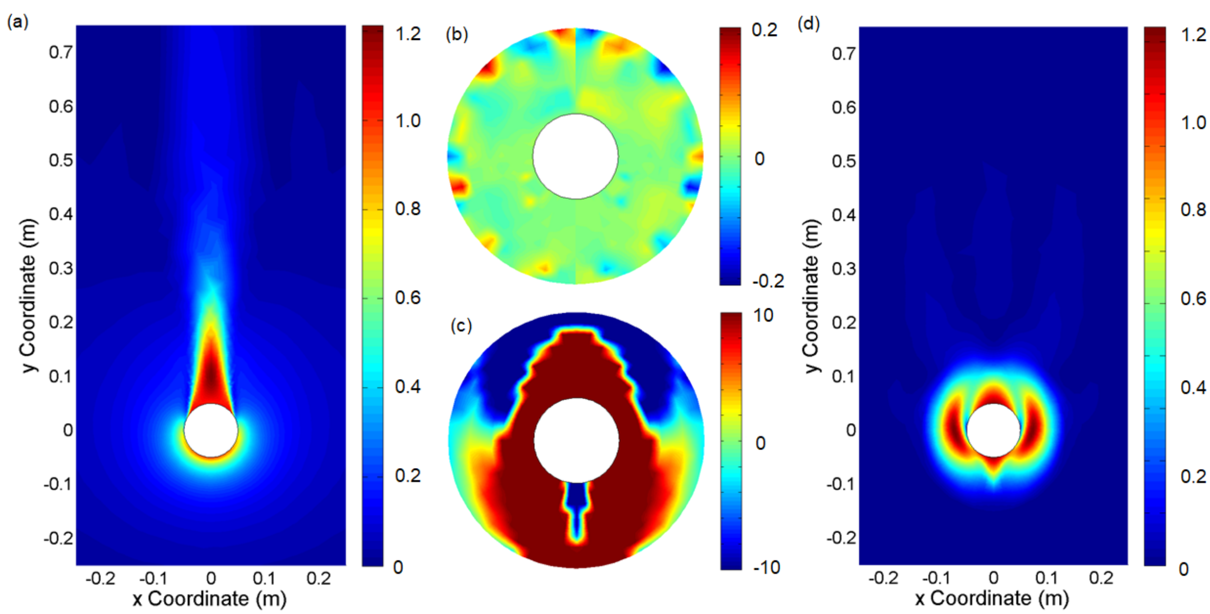

FIG. 6: (a - left) LW in the flow surrounding the uncloaked cylinder at Re=100. (b - top center) Volumetric force (normalized by $F_{V,0}$) in the x direction necessary to achieve cloaking as determined by optimization. (c - bottom center) Volumetric force (normalized by $F_{V,0}$) in the y direction necessary to achieve cloaking as determined by optimization. (d - right) LW in the flow surrounding the cloaked cylinder at Re=100.

CFD simulations with RANS corrections confirm that effective drag reduction is possible with forced Stokes flows. The simulations specifically used the $k-\varepsilon$ model in the COMSOL turbulent flow module [20]. Using parametric continuation, the uncloaked cylinder solution is found by gradually turning off the volumetric force. Figure 5 illustrates that mechanical power dissipation is decreased more than four-fold.

Convergence in FEM solvers is difficult to achieve in these optimization simulations for a number of reasons. At any iteration or mutation of a trial solution, the algorithm could test a configuration that generates a large gradient in the Lorentz force distribution. This is particularly troublesome when the gradient is near the solid core as the large force may demand a large flow velocity very close to the wall boundary, and rectifying that flow velocity gradient within a single element cannot be done. Forced Stokes solutions offer a nice technique for accelerating convergence, since the expected velocity profile is known. In the next section, these issues were addressed by prescribing initial conditions on the Lorentz force that did not have large gradients near the boundaries. This almost guaranteed a converged solution on the flow field for the initial guess, and the adjoint optimization scheme Method of Moving Asymptotes (MMA)

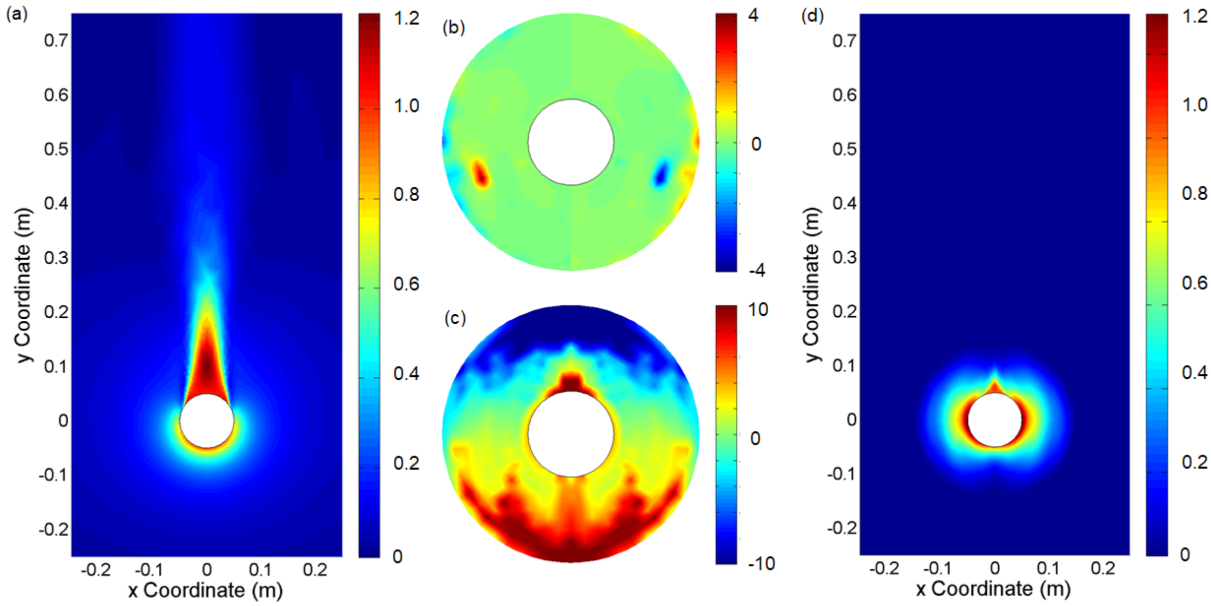

FIG. 7: (a - left) LW in the flow surrounding the uncloaked cylinder at Re=10^7. (b - top center) Volumetric force (normalized by $F_{V,0}$) in the x direction necessary to achieve cloaking as determined by optimization. (c - bottom center) Volumetric force (normalized by $F_{V,0}$) in the y direction necessary to achieve cloaking as determined by optimization. (d - right) LW in the flow surrounding the cloaked cylinder at Re=10^7.

would make incremental adjustments from that converged solutions. This, typically, prevented large gradients from appearing trial solutions throughout the simulation. Spanwise symmetry was also enforced to reduce the size of the solution space.

B. Wake Elimination via Force Distribution Optimization

The volumetric force in the cloak envelope necessary to eliminate the wake can also be visualized using optimization techniques. We first construct a model of a cylinder in cross flow in COMSOL Multiphysics and prescribe an annular region in which an unknown body force may be applied. We then simulate the flow and allow COMSOL to vary the volumetric forces in the x and y directions within $\pm F_{V,0}$. These fields are continuous, and can be modified based on the optimization mesh precision. Figures 6 through 7 illustrate the results of some optimization runs at Reynolds numbers varying from 100 to 10^7. The objective function for the optimization is the Domain Wide Wake (DWW) defined below

$$DWW \equiv \frac{1}{V_f} \iiint_{V_f} LW dV \tag{16}$$

where V_f is the volume of the domain excluding the regions of the Lorentz Force.

All of these figures illustrate that cloaking is achieved mainly through the control of the volumetric force in the y direction. Furthermore, these results show that effective cloaking can be achieved by accelerating the flow upstream of the object and immediately downstream of the object, and decelerating the flow farther downstream. These observations inform design decisions when considering ways to impart a volumetric force on the flow. Another observation of note: the distribution of volumetric force necessary to achieve hydrodynamic cloaking (relative to $F_{V,0}$) does not change considerably beyond Re= 10^3. This suggests that, beyond a certain free-stream velocity threshold, a single configuration of an active cloaking device may be able to accommodate all flow speeds, only with greater power consumption.

It is important to note that these configurations are somewhat different than those in the analytical cloaking investigation. This simply illustrates that there are an infinite number of solutions to achieve hydrodynamic cloaking. The key will be finding a configuration that minimizes the power consumption of a practical device.

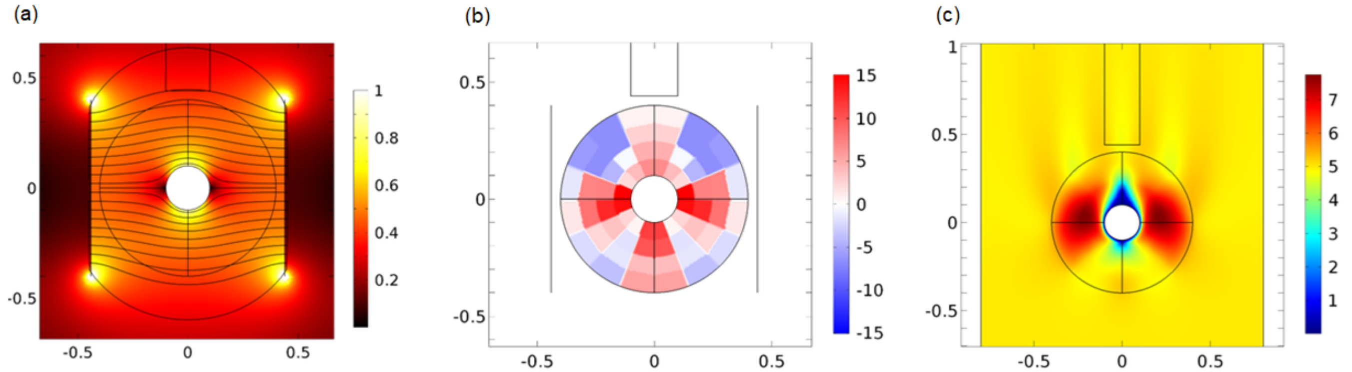

FIG. 8: Optimized configuration of an MHD array surrounding a cylindrical core for wake elimination. This differs from the configuration in figures 6 and 7 because the force production is discretized into cells (possibly by the presence of out-of-plane inductors). (a - left) illustrates the current lines and current density in the flow field of the cload. (b - right) shows the magnetic field magnitudes in the various cells of the array. (c - right) shows the flow velocity of the wake-minimized, cloaked field.

III. IMPLEMENTATION OF ZERO WAKE FLOWS WITH MAGNETOHYDRODYNAMIC FORCES

As the previous sections show, identifying configurations of a volumetric force for the purpose of wake elimination can be done a number of different ways. The true challenge is finding techniques to impart such a volumetric force on the flow in the near field of an object. The most promising avenue to achieve this for conducting fluids is Magnetohydrodynamics (MHD), and it may be implemented in a number of ways.

A. Magnetohydrodynamic Flow Control Inspired by Metamaterials

In the spirit of the work of Pendry [6] and Cummer [7] we may consider hydrodynamic cloaking device designs inspired by metamaterial cloaks in electromagnetics and acoustics. We choose to impart the body force using magnetohydrodynamics, and the cells in the MHD flow control array will contain different magnetic fields from idealized infinite inductors. In the cross-stream direction, we will impart an electric field to create the Lorentz force. Such an array and its properties are illustrated in figure 8, where the fluid is assumed to be oceanic saltwater, whose typical electrical conductivity is in the range of $1 - 10$ S/m.. On the left, the distribution of electric current throughout the 2D system is shown. The current density is high at the tips of the electrodes (as expected) but the current in the MHD array is significant enough to generate a usable Lorentz force. In the middle panel, the optimized grid of magnetic field cells is shown. The magnetic field magnitude in each cell is chosen to minimize the wake downstream from the object. Finally, in the right panel, the flow field around the cylinder

B. Magnetohydrodynamic Flow Control with Large Magnetic Field Domains

In place of a metamaterial-inspired design, larger, bulk Lorenz domains may be used to control the flow around the cylinder. Figures 6 through 7 show consistent regions in which the body force differs to achieve cloaking among a number of Reynolds numbers: an accelerated upstream region, an accelerated region near the core (especially along the immediately downstream surface), and a decelerated downstream region. More plainly, the aforementioned computational results suggest that much of the wake can be eliminated by controlling the flow in smaller, discrete regions. A design analogy using magnetohydrodynamics is illustrated in figure 9 below, where these important discrete regions will be modeled within the three circles downstream from the core and the ellipse upstream from the core. The vertical lines (except for the midline) represent the location of electrodes, where the upstream electrode voltage is denoted V_{us}, the center electrode voltage is denoted V_c, and the downstream electrode voltage is denoted V_{ds}. Similarly, the magnetic field magnitudes are denoted as $B_{ds,1}$ (middle downstream inductor), $B_{ds,2}$ (outbound downstream inductors), B_c (center upstream inductor), and B_{us} (upstream inductor). Note that these discrete regions, in practice, could be thin-wired, large-pitch inductor coils to minimize their effect on the flow. The influence of the flow impedance from the coils or other magnetic-field-imparting device is left to future work.

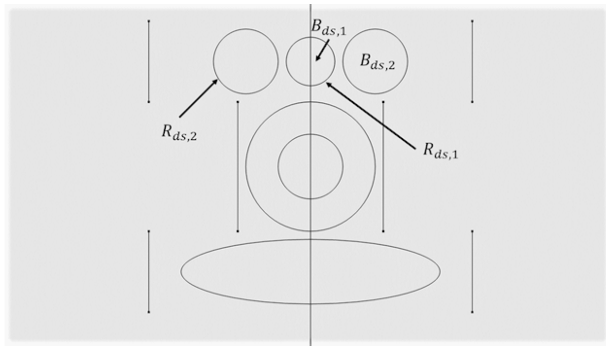

FIG. 9: Schematic of the magnetohydrodynamic cloaking device for 2D flow around a cylinder. The only alterations are in the downstream magnetic fields. In place of a single ellipse, three circles now help to control the flow. $R_{ds,1} = 0.75R_c$ and $R_{ds,2} = R_c$. The off-axis domains are displaced by $2R_c$.

The results of optimizing the electric and magnetic field parameters for this system are shown in figure 10

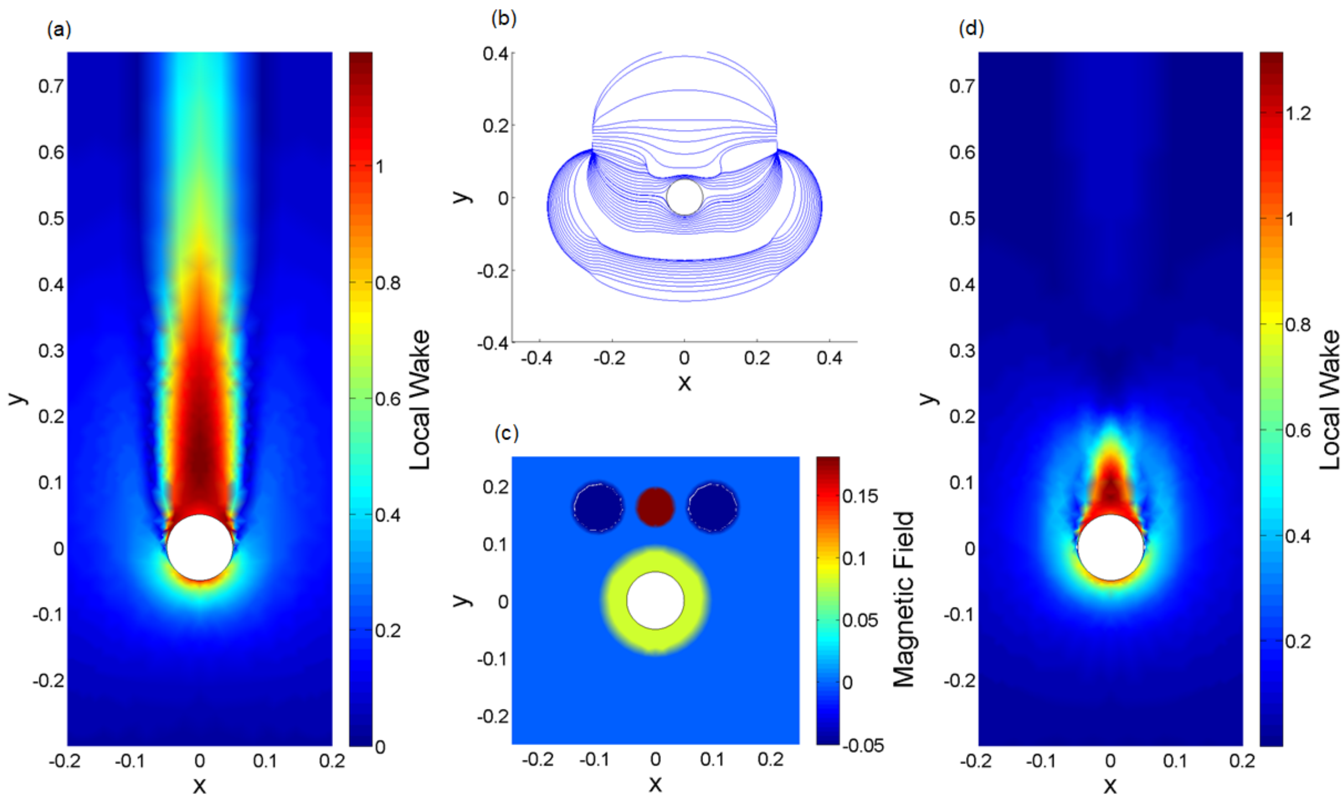

FIG. 10: Cloaking results using a modified MHD array to simulate the results of the general body force optimization. (a - left) The uncloaked 2D flow around a cylinder at Reynolds number 10,000. (b - top-middle) Electrical current lines around the cylindrical core due to optimized electrode potential. (c - bottom-middle) Optimized out-of-plane magnetic fields in Tesla. (d - right) Resulting local wake of the cloaked configuration.

The body force resulting from the electric and magnetic fields shown in figure 10 is shown below in figure 11, and the optimized parameter values are summarized in table I.

TABLE I: Optimized values for electromagnetic field parameters in figure 11

Parameter	Optimized Value	Unit
V_{us}	3.87	V
V_c	2.28	V
V_{ds}	32.6	V
B_{us}	0	mT
B_c	80.8	mT
B_{ds}	130	mT
$B_{ds,2}$	-50	mT
Wake Reduction	81.3%	N/A

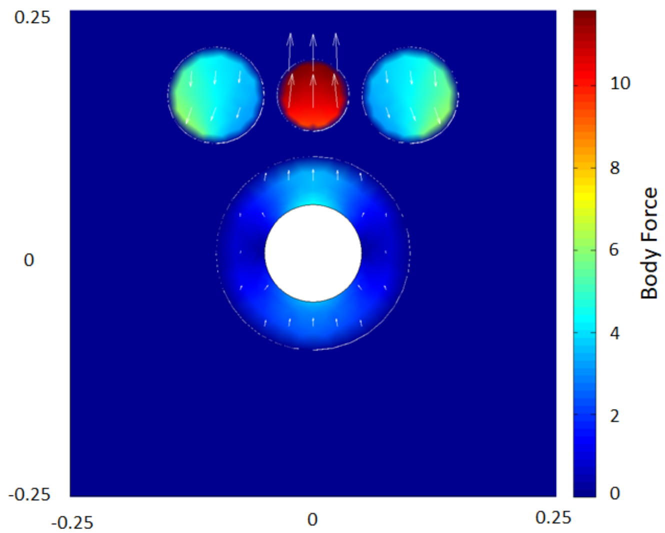

FIG. 11: Body force resulting from the first MHD configuration. The body force magnitude is normalized by $F_{B,0}$.

With this modified configuration of magnetic field domains and electrodes, the following parameters were identified by the optimization algorithm yielding the minimum wake.

It is important to note that, though the optimal upstream magnetic field is zero, the upstream electrodes were useful in changing the electric field passing through the other Lorentz domains. Moreover, these discrete regions were capable of eliminating over 80% of the wake in this otherwise turbulent (Re=10^5) flow with small voltages and magnetic fields.

IV. CONCLUSIONS

A path to hydrodynamic cloaking of bodies in a conducting fluid using magnetohydrodynamics has been computationally developed. Using COMSOL multiphysics and its optimization capabilities, general distributions of body forces for cloaking cylinders at a wide array of Reynolds numbers have been identified. These distributions informed the configuration of an MHD array around a cylinder to achieve an approximate analogue of the desired body force using a practical avenue. Ultimately, the magnetic fields and electrode voltages necessary to cloak a cylinder at a Reynolds number of 10,000 have been calculated using COMSOL's optimization MMA algorithm and the $k - \varepsilon$ turbulence model.

There are many opportunities for future work in the wake of these results. Developing and modeling a practical feature for imparting the desired magnetic fields in the system is a clear priority. One may use coarse inductors capable of carrying large current, but the flow resistivity of the inductors must be taken into account when identifying the necessary Lorentz force to eliminate the system wake. This could be accomplished by an empirical study of transverse flow through coils of various wire diameter, major diameter, and pitch, identifying the pressure drop due to their presence. Other possible advancements include different core geometries, different body-force-generating designs to achieve the optimal envelope configuration, and power minimization of any proposed systems.

V. ACKNOWLEDGMENTS

This work was supported by the Office of Naval Research (ONR) through the Naval Undersea Research Program, award no. N00014-13-1-0743, and partially through the Multidisciplinary University Research Initiative (MURI), award no. N00014-13-1-0631. Dean Culver acknowledges partial financial support of the Naval Research Enterprise Internship Program (NREIP), Department of the Navy. The authors would like to thank Abraham Varghese and other personnel of the Naval Undersea Warfare Center in Newport, Rhode Island for stimulating discussions.

[1] E.W. Graham. A drag reduction method for wings of fixed plan form. *Journal of the Aeronautical Sciences*, 19:823–825, 1952.
[2] A. Ferri and J. Clarke. On the use of interfering flow fields for the reduction of drag at supersonic speeds. *Journal of the Aeronautical Sciences*, 24:1–18, 1957.
[3] P. Chang. Drag reduction of an airfoil by injection of sound energy. *Journal of the Aeronautical Sciences*, 28:742–743, 1961.
[4] G.F. Anderson and S.P. Sutera. Drag reduction on bodies of revolution by use of area suction. *AIAA Journal*, 3:1970–1972, 1965.
[5] H. Choi, P. Moin, and J. Kim. Active turbulence control for drag reduction in wall-bounded flows. *Journal of Fluid Mechanics*, 262:75–110, 1994.
[6] J. Pendry, D. Schurig, and D. Smith. Controlling electromagnetic fields. *Science*, page 312, 2006.
[7] S. Cummer and D. Schurig. One path to acoustic cloaking. *New Journal of Physics*, page 45, 2007.
[8] Y. Urzhumov and D. Smith. Fluid flow control with transformation media. *Physical Review Letters*, 107:074501:1–4, 2011.
[9] Y. Urzhumov and D. Smith. Flow stabilization with active hydrodynamic cloaks. *Physical Review E*, 86:056313:1–5, 2012.
[10] P. Bowen, D. Smith, and Y. Urzhumov. Wake control with permeable multilayer structures: the spherically symmetric case. *Physical Review E*, 92, 2015.
[11] B. Popa and S. Cummer. Non-reciprocal and highly nonlinear active acoustic metamaterials. *Nature Communications*, 5:3398, 2014.
[12] B. Popa and S. Cummer. Negative refraction of sound. *Nature Materials*, 14:363–364, 2014.
[13] B. Popa and S. Cummer. Preserving omnidirectionality in optimized asymmetric transformation optics designs. *Journal of Optimization*, 18:044018, 2016.
[14] S. Cummer. *Nonlinear, Tunable and Active Metamaterials*. Springer, 2015.
[15] S. Cummer, J. Christensen, and A. Alu. Controlling sound with acoustic metamaterials. *Nature Reviews*, 2016.
[16] L. Zigoneanu and S. Cummer. Three-dimensional broadband omnidirectional acoustic ground cloak. *Nature Materials*, 13:352–355, 2014.
[17] J. Barrett and S. Cummer. Design and full characterization of planar active magnetic rf metamaterials. *IEEE Antennas and Wireless Propagation Letters*, 14:943–946, 2015.
[18] S. Kim and Lee C.M. Control of flows around a circular cylinder: suppression of oscillatory lift force. *Fluid Dynamics Research*, 29:47–63, 2001.
[19] B.H. Dennis and G.S. Dulikravich. Optimization of magneto-hydrodynamic control of diffuser flows using micro-genetic algorithms and least-squares finite elements. *Finite Elements in Analysis and Design*, 37:349–363, 2001.
[20] *CFD Module User's Guide*.